PREPARATION AND CHARACTERIZATION OF POLY(ETHYLENE OXIDE)/LITHIUM MONTMORILLONITE COMPOSITES

M. Erceg[1*], M. Omazić[1], N. S. Vrandečić[1], I. Banovac[1]

[1]*Faculty of Chemistry and Technology, Department of Organic Technology, University of Split, Teslina 10/V, 21000 Split, Croatia*
**merceg@ktf-split.hr*

Keywords: poly(ethylene oxide), lithium montmorillonite, polymer electrolytes, crystallinity

Abstract
Poly(ethylene oxide)/lithium montmorillonite (PEO/LiMMT) composites were prepared by mixing and ultrasonication PEO and LiMMT in water. Characterization of PEO/LiMMT composites was performed by differential scanning calorimetry (DSC), Fourier transform infrared spectroscopy (FT-IR) and non-isothermal thermogravimetry (TGA). DSC and TGA reveal that higher loadings of LiMMT significantly influence the crystallinity, melting temperatures and thermal stability of PEO, respectively. Glass transition temperatures of PEO do not change with addition of LiMMT. FT-IR analysis shows that the helical structure of PEO chains is distorted in PEO/LiMMT composites. Changes of activation energy in composites compared to pure PEO indicate possible changes in the mechanism of the non-isothermal degradation of PEO due to addition of LiMMT.

1 Introduction

Poly(ethylene oxide) (PEO) as solid polymer electrolyte in lithium polymer batteries has many advantages over its liquid counterparts or organic solutions due to the ease of processing, stable electrochemical characteristics and excellent mechanical properties [1]. However, since ionic conductivity primarily takes place in the amorphous phase, high crystallinity of PEO limits the lithium ion transport resulting in a poor ionic conductivity of PEO electrolytes at room temperatures (usually lower than 10^{-6} Scm^{-1} [2]). One of the ways to reduce the crystallinity of PEO is the incorporation of inorganic nanophases such as nanoclays in the PEO matrix. This investigation is focused on the preparation and characterization of PEO composites with lithium montmorillonite (LiMMT) as nanoclay in order to establish influence of LiMMT on crystallinity, thermal stability and thermal degradation of PEO.

2 Materials and testing methods

2.1 Materials and sample preparation

PEO powder with viscometric average molecular weight of 300.000 was purchased from Sigma Aldrich. LiMMT was prepared by ion-exchange from natural montmorillonite (Cloisite®Na^+, Southern Clay Products Inc., USA) and lithium chloride (Kemika, Croatia). Ion-exchange has been carried out by suspending 15.0 g of Cloisite®Na^+ in 400 cm^3 of 1.0 $moldm^{-3}$ LiCl solution in water. The suspension was stirred with magnetic stirrer for 48 hours at 40 °C. Mixture was then centrifuged at 5000 rpm until clear separation was obtained and supernatant decanted. Series of washings with de-ionized water and centrifugation were

performed until chloride ions were completely removed (tested using $AgNO_3$ solution). Obtained residue is LiMMT. LiMMT was then dried in oven for 5 hours at 120 °C and then in vacuum oven for 48 hours at 100 °C.
PEO/LiMMT composites with compositions 100/0, 99/1, 97/3, 95/5, 93/7, 90/10, 85/15, 75/25, 65/35 and 50/50 by weight (where 100/0 represents pure PEO) were prepared. Certain amounts of LiMMT, depending on the sample composition, were dispersed in 100 mL of distilled water by vigorous mechanical stirring for 2 hours and ultra-sonication at 160 W at room temperature for 30 min. In the each obtained dispersion certain amount of 2 % wt/v aqueous solution of PEO was added and stirred overnight. The resulting dispersions were then poured into Petri dishes and PEO/LiMMT films were obtained by evaporating water at 40 °C and drying in vacuum oven at 40 °C for 24 hours.

2.2 Testing methods
Differential scanning calorimetry (DSC) measurements were performed on Mettler-Toledo 823^e calorimeter in nitrogen atmosphere (30 cm^3min^{-1}). Samples of 14.7±1.5 mg were encapsulated in aluminum pans, cooled to -90 °C at the cooling rate of 20 °$Cmin^{-1}$, kept at -90 °C for 10 minutes and heated to 120 °C at the heating rate of 20 °$Cmin^{-1}$. The characteristic glass transition temperatures, i.e. extrapolated onset temperature (T_{eig}), midpoint temperatures (T_{mg}) and extrapolated end temperatures (T_{efg}), the characteristic melting temperatures, i.e. extrapolated onset temperatures (T_{eim}), peak temperatures (T_{pm}) and the extrapolated end temperatures (T_{efm}) as well as the melting enthalpy (ΔH_m) were determined from DSC curves. The degree of crystallinity (X_c) is directly proportional to ΔH_m for a crystalline polymer under the same condition of DSC experiment and is calculated according to equation (1):

$$X_c(\%) = \frac{\Delta H_m}{\Delta H_0 \cdot w} \cdot 100 \qquad (1)$$

where ΔH_0 is the melting enthalpy per unit weight of the 100 % crystalline PEO, which is 205 Jg^{-1} [3] and w the weight fraction of PEO in the sample. The apparatus was calibrated with an indium standard and before operating the system was stabilized for 1 hour.

IR spectroscopy was performed on a Perkin-Elmer Spectrum One FT-IR spectrometer. FT-IR spectrograms (average of 40 scans) were recorded using HATR (Horizontal Attenuated Total Reflectance) technique, ZnSe 45° crystal, in the range of wave numbers between 650 and 4000 cm^{-1}, with a spectral resolution of 4 cm^{-1}. Samples in the form of films were cut in the rectangles (6.0 x 1.5 mm) in order to fully cover the surface of ZnSe crystal.

The thermal degradation (sample mass 7.8±1.2 mg) was performed by the non-isothermal thermogravimetry (TGA). TGA was carried out in the temperature range from 50 to 500 °C using a Perkin-Elmer Pyris 1 TGA. The nitrogen flow rate was 30 cm^3min^{-1} and the heating rates were 2.5, 5, 10 and 20 °$Cmin^{-1}$. The onset degradation temperature ($T°$), the temperature at the maximum degradation rate (T_{max}), the maximum degradation rate (R_{max}) and the residual mass (m_f) were calculated from the TG curves. Before operating, the system was stabilized for 1 hour.

2.3 Kinetic analysis
Isoconversional methods are considered as the most reliable methods for the calculation of activation energy (E) and the dependence of E on conversion, α [4, 5]. Therefore, in this work isoconversional Flynn-Wall-Ozawa (FWO) [6, 7] (equation 2) and Friedman (FR) [8] (equation 3) methods were used:

$$\log\beta = \log\frac{AE_{FWO}}{Rg(\alpha)} - 2{,}315 - 0{,}4567\frac{E_{FWO}}{RT} \quad (2) \qquad \ln\left[\beta\frac{d\alpha}{dT}\right] = \ln A + \ln f(\alpha) - \frac{E_{FR}}{RT} \quad (3)$$

where β is the linear heating rate, A pre-exponential factor, R is the general gas constant, T is the absolute temperature, $f(\alpha)$ and $g(\alpha)$ are differential and integral form of the kinetic model and α is conversion defined as the ratio $(m_0\text{-}m)/(m_0\text{-}m_f)$, where m_0, m and m_f are initial, actual and residual mass of the sample. For α=const., the plots logβ vs. $1/T$ and ln[βdα/dT] vs. $1/T$ obtained from α-T curves recorded at several heating rates should be straight lines whose slope allows calculation of E by means of FWO (E_{FWO}) and FR (E_{FR}) method, respectively.

3 Results and discussion

3.1 Differential scanning calorimetry analysis

Normalized DSC heating curves of all analyzed samples are shown in Figure 1 and characteristics of DSC curves, T_{eig}, T_{mg}, T_{efg}, T_{eim}, T_{pm}, T_{efm}, ΔH_m and X_c are given in Table 1.

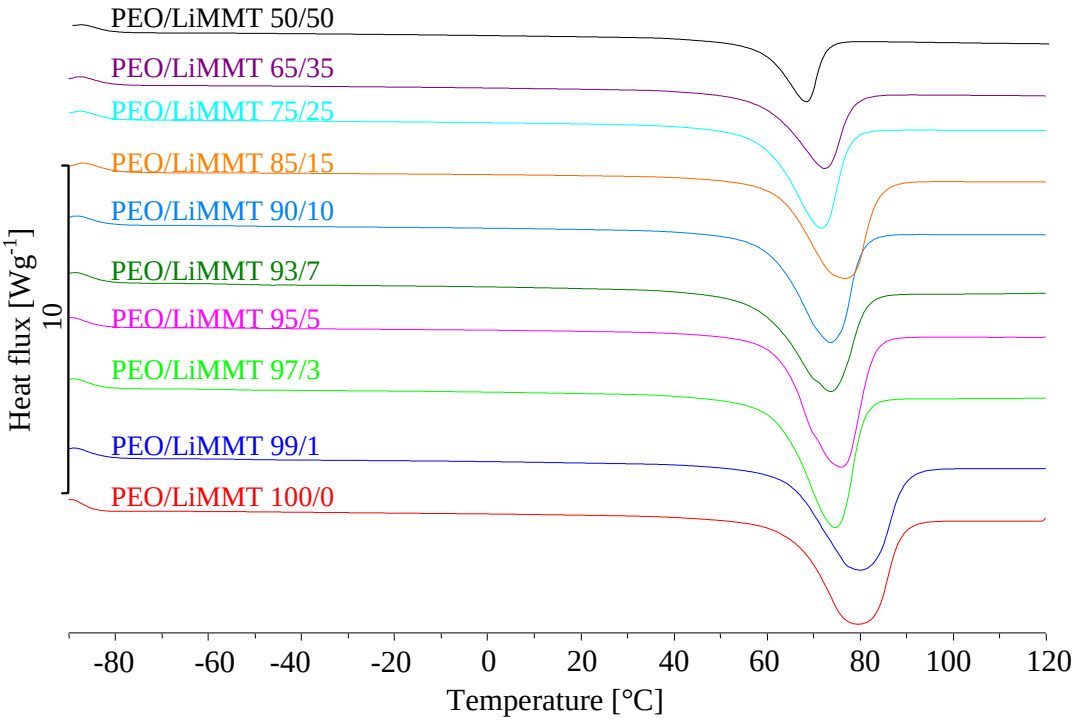

Figure 1. Normalized DSC heating curves of PEO and PEO/LiMMT composites.

PEO/LiMMT	T_{eig} [°C]	T_{mg} [°C]	T_{efg} [°C]	T_{eim} [°C]	T_{pm} [°C]	T_{efm} [°C]	ΔH_m [Jg^{-1}]	X_c [%]
100/0	-59	-54	-48	65	78	89	177.5	86.6
99/1	-57	-53	-48	63	78	89	167.6	82.6
97/3	-58	-54	-49	62	77	85	158.8	79.9
95/5	-56	-51	-46	64	79	89	152.8	78.5
93/7	-57	-53	-49	58	72	81	149.1	78.2
90/10	-57	-53	-49	60	72	80	143.2	77.6
85/15	-56	-52	-47	61	74	82	132.9	76.3
75/25	-57	-52	-47	59	70	77	117.8	76.6
65/35	-54	-53	-48	59	71	78	92.2	69.2
50/50	-59	-54	-48	58	67	72	58.7	57.3

Table 1. DSC data for PEO and PEO/LiMMT composites.

All samples (Figure 1) show one endothermic peak which represents melting of the crystalline phase in PEO. It is important to emphasize that DSC characteristics are taken from the first heating scan, not from second one as usual, in order to evaluate samples properties as prepared. The glass transition temperatures of PEO, expressed as T_{eig}, T_{mg} and T_{efg}, do not change with addition of LiMMT indicating that flexibility of PEO chains do not change in composites. The melting temperatures of crystalline PEO phase, expressed as T_{eim}, T_{pm} and T_{efm} shift towards lower temperatures with increasing LiMMT content over 5 wt. %, where shift of T_{pm} and T_{efm} is more pronounced compared to T_{eim} (Table 1). The melting enthalpies, ΔH_m of samples decrease linearly with increase of LiMMT in composites (Table 1). The proportion of PEO crystalline phase, i.e. the degree of crystallinity, X_c was calculated according to equation (1). Addition of LiMMT up to 5 wt. % decreases X_c for 8 % and then X_c remains almost constant up to addition of 25 wt. % of LiMMT when sharp decrease of X_c occurs. X_c decreases from 87 % in pure PEO to 57 % in composite with 50 wt. % of LiMMT. Obviously, X_c decreases with increasing LiMMT loading, because at higher loadings LiMMT platelets more intensively stop the growth of PEO crystalline lamellae.

3.2 FT-IR analysis

FT-IR spectroscopy is powerful tool for providing information regarding the difference between polymer and polymer/clay composites. FT-IR spectra of pure PEO and PEO/LiMMT 50/50 are shown in Figure 2. Pure PEO is, as mentioned before, highly crystalline polymer with macromolecules in the helical (7_2 helix) conformation [9, 10]. The peaks near 945 cm^{-1} and 840 cm^{-1} are generally related to the CH_2 rocking vibrations in the gauche conformation required for the helical conformation of PEO. These peaks can be observed in FT-IR spectra of pure PEO, indicating that pure PEO really is in helical conformation. As the amount of LiMMT increases in PEO/LiMMT composites, the intensity of peaks at 945 cm^{-1} and at 840 cm^{-1} decreases while above 35 wt. % of LiMMT peak at 945 cm^{-1} completely disappears. This indicates that in PEO/LiMMT composites the helical structure of PEO is distorted/perturbed.

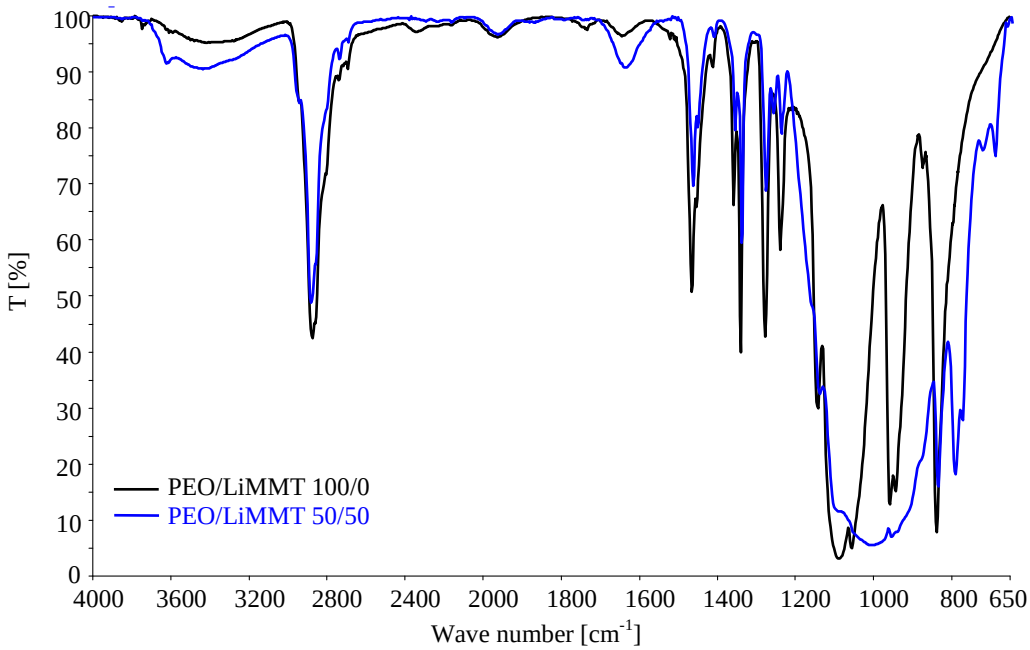

Figure 2. FT-IR spectra of pure PEO and PEO/LiMMT 50/50 composite.

Moreover, presence of three sharp peaks in the region of 1200-1000 cm^{-1} (C-O-C stretching at 1144 cm^{-1} and at 1090 cm^{-1} and C-O stretching at 1058 cm^{-1}) confirms the existence of crystalline phase in PEO. However, in PEO/LiMMT composites, these peaks are getting broader and merge into one broad peak, especially at higher loadings of LiMMT, as can be seen in Figure 2 for PEO/LiMMT 50/50 sample. This behaviour also indicates the change of PEO crystallinity in PEO/LiMMT composites, what is in accordance with DSC results.

3.3 Thermogravimetric analysis

Non-isothermal degradation of all samples was performed in the temperature region 50-500 °C at four heating rates (2.5, 5, 10 and 20 °$Cmin^{-1}$) in order to establish the influence of LiMMT on the thermal stability and obtain data for the kinetic analysis of the degradation process. TG curves of all analysed samples at the heating rate 10 °$Cmin^{-1}$ are shown in Figure 3. In this temperature region, LiMMT is thermally stabile and observed mass loss (approximately 5 wt. %) is attributed to its dehydratation and dehydroxylation.

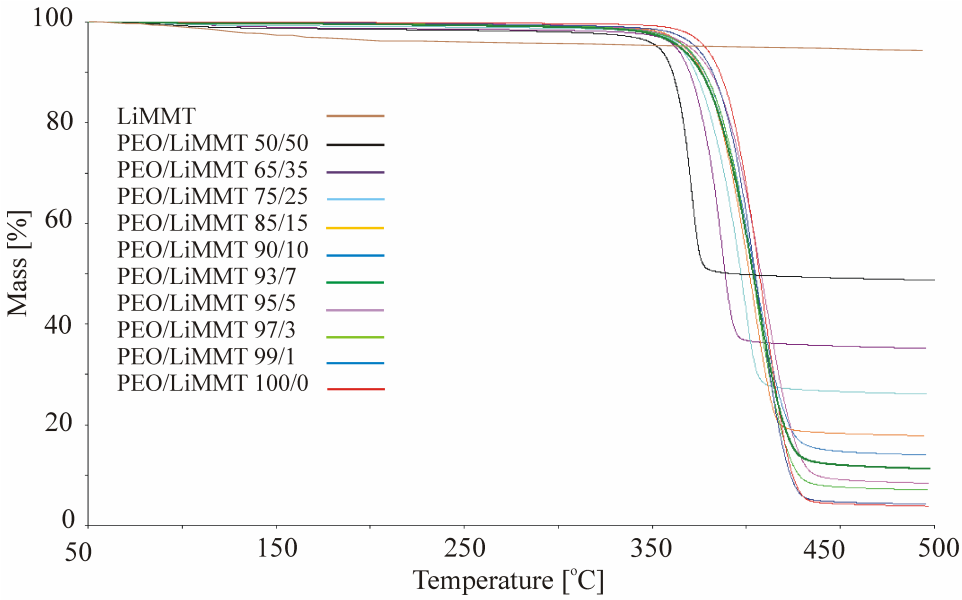

Figure 3. TG curves of PEO/LiMMT composites at the heating rate 10 °C/min.

Thermal degradation of both pure PEO and PEO/LiMMT composites occurs through one degradation step in the temperature range 310-450 °C, depending on the sample composition and the heating rate. In order to establish the influence of LiMMT content on the thermal stability of PHB, the onset degradation temperatures ($T°$) and the temperatures at the maximum degradation rate (T_{max}) were determined from non-isothermal thermogravimetry. The results are shown in Table 2. $T°$ values for PEO/LiMMT composites up to 10 wt. % LiMMT are slightly lower compared to pure PEO, while at higher LiMMT amounts $T°$ values are significantly lower compare to pure PEO. The similar behavior is observed for T_{max} values. It should be emphasized that the values of $T°$ and T_{max} for the sample with 50 wt. % Li-MMT are up to 30 °C and 40 °C lower (depending on the heating rate) than for the original PEO, respectively. This means that addition of LiMMT lowers the thermal stability of PEO although it is generally believed that introduction of inorganic components into organic materials improves their thermal stabilities due to the physical protective barrier and delayed volatization of degradation products [11]. Similar behavior has been observed for some other

polymer composites and nanocomposites, but it is still not clear what mechanism causes this reduction. Residual mass, m_f (Figure 3, Table 2) increases linearly with addition of LiMMT due to thermal stability of LiMMT in this temperature range. The maximum degradation rate (R_{max}) of PEO (Table 2) lowers by the addition of LiMMT up to 10 wt. % and then increases, so that samples with 35 and 50 wt. % show higher R_{max} values than the original PEO. These changes in R_{max} values indicate possible changes in the mechanism of thermal degradation of PEO in the presence of LiMMT.

β [°Cmin^{-1}]	Values	PEO/LiMMT									
		100/0	**99/1**	**97/3**	**95/5**	**93/7**	**90/10**	**85/15**	**75/25**	**65/35**	**50/50**
2.5	**T°[°C]**	357	358	356	355	356	356	354	351	347	338
	T_{max}[°C]	381	381	379	378	381	381	375	373	362	348
	m_f [%]	4	6	8	9	11	14	19	25	36	49
	R_{max} [°Cmin^{-1}]	8	7	6	6	6	6	6	8	8	9
5	**T°[°C]**	380	373	367	369	371	373	364	368	365	351
	T_{max}[°C]	401	394	394	394	399	396	388	387	380	362
	m_f[%]	4	5	8	9	11	14	18	27	35	48
	R_{max} [°Cmin^{-1}]	14	14	11	11	10	11	11	16	18	17
10	**T°[°C]**	388	386	383	384	385	381	380	380	373	362
	T_{max}[°C]	409	408	405	409	408	405	404	400	387	371
	m_f[%]	4	5	7	8	11	14	18	26	35	47
	R_{max} [°Cmin^{-1}]	27	26	24	22	21	21	24	27	32	36
20	**T°[°C]**	398	395	395	397	397	396	395	398	384	377
	T_{max}[°C]	420	418	419	421	420	420	420	408	400	387
	m_f[%]	3	6	7	8	12	14	18	26	35	49
	R_{max} [°Cmin^{-1}]	52	49	43	41	41	41	44	44	59	67

Table 2. Characteristics of the non-isothermal degradation of all analyzed samples.

Kinetic analysis was performed by isoconversional Flynn-Wall-Ozawa and Friedman methods in order to determine the activation energy and its dependence on conversion. Results are given in Table 3.

PEO/LiMMT	E_{FWO} [kJmol^{-1}]	r^2	E_{FR} [kJmol^{-1}]	r^2
100/0	209±4	0.99036	210±11	0.98846
99/1	188±4	0.99214	190±9	0.99085
97/3	174±4	0.99596	177±8	0.98937
95/5	160±3	0.99790	161±5	0.99730
93/7	177±1	0.99783	176±3	0.99403
90/10	183±2	0.98656	185±5	0.98514
85/15	149±4	0.99624	155±4	0.99320
75/25	176±4	0.99169	176±13	0.99388
65/35	181±5	0.98327	189±11	0.98187
50/50	169±6	0.99421	184±13	0.98518

Table 3. Average activation energy values obtained by Flynn-Wall-Ozawa and Friedman methods.

If *E* is roughly constant over the whole conversion range it is likely that process is dominated by a single reaction step [12]. It is well established that PEO degradation occurs by the

random-chain scission of C-O and C-C bonds [13]. The nearly constant E_{FWO} and E_{FR} values for pure PEO (Table 3) suggest that degradation kinetics is essentially limited by a single reaction step, where value of around 210 kJmol^{-1} corresponds to above mentioned degradation mechanism. PEO/LiMMT composites show lower E_{FWO} and E_{FR} values compared to pure PEO, while constancy over the whole conversion range is remained. This indicates that degradation kinetics in PEO/LiMMT composites is also governed by a single reaction step but probably different from one in pure PEO. However, in order to fully clarify this issue more advanced kinetical analysis and more sophisticated analytical equipment should be used.

4 Conclusions

PEO/LiMMT composites up to 50 wt. % of LiMMT were prepared in order to establish the influence of LiMMT on the crystallinity, glass transition and melting temperatures, thermal stability and non-isothermal degradation of PEO. Only higher loadings of LiMMT significantly influence the crystallinity, melting temperatures and thermal stability of PEO, respectively. Addition of 50 wt. % of LiMMT reduces PEO crystallinity for almost 30 %, melting temperature for more than 10 °C and thermal stability for 20-30 °C, depending on the heating rate. Glass transition temperatures of PEO do not change with addition of LiMMT. FT-IR analysis also proofs that more pronounced change in conformation and crystallinity of PEO occurs at higher LiMMT loadings. Flynn-Wall-Ozawa and Friedman methods were used to calculate the activation energy of the non-isothermal degradation of pure PEO and PEO/Li-MMT composites. Activation energy of the non-isothermal degradation of PEO/Li-MMT composites is lower compared to pure PEO indicating changes in the degradation mechanism.

References

[1] Chien-Shiun L., Wei-Bin Ye. Enhanced Ionic Conductivity in Poly(ethylene oxide)/Layered Double Hydroxide Nanocomposite Electrolytes. *Journal of Polymer Research*, **10**, pp. 241-246 (2003).

[2] Al-Ramadin Y. Optical properties of poly(vinyl chloride)/poly(ethylene oxide) blend. *Optical Materials*, **14**, pp. 287-290 (2000).

[3] Zheng S., Nie K., Guo Q. Miscibility and phase separation in blends of phenolphthalein poly(aryl ether ketone) and poly(ethylene oxide): a differential scanning calorimetric study, *Thermochimica Acta*, **419**, pp. 267-274 (2004)

[4] Vyazovkin S., Lesnikovich, A. I. An approach to the solution of the inverse kinetic problem in the case of complex processes: Part 1. Methods employing a series of thermoanalytical curves, *Thermochimica Acta*, **165**, pp. 273-280 (1990)

[5] Vyazovkin S., Sbirrazzuoli N. Isoconversional Kinetic Analysis of Thermally Stimulated Processes in Polymers. *Macromolecular Rapid Communications*, **27**, pp. 1515–1532 (2006).

[6] Ozawa T. A new method of analysing thermogravimetric data. *Bulletion of the Chemical Society of Japan*, **38**, pp. 1881-1889 (1965).

[7] Flynn J. H., Wall L. A. General treatment of the thermogravimetry of polymers. *Journal of Research of the National Bureau of Standards*, **70A**, pp. 487-523 (1966).

[8] Friedman H. L. Kinetics of thermal degradation of char-forming plastics from thermogravimetry. Applications to a phenol plastic. *Journal of Polymer Science*, **6C**, pp. 183-195 (1963).

[9] Shen Z., Simon G. P., Cheng Y. Saturation ratio of poly(ethylene oxide) to silicate in melt intercalation nanocomposites. *European Polymer Journal*, **39**, pp. 1917-1924 (2003).

[10] Gnanou Y., Fontanille M. *Organic and Physical Chemistry of Polymers*. John Wiley&Sons, Inc., Hoboken, New Jersey (2008).
[11] Wu D., Wu L., Wu L, Zheng M. Rheology and thermal stability of polylactide/clay nanocomposites. Poylmer Degradation and Stability, **91**, pp. 3149-3155 (2006).
[12] Vyazovkin S., Burnhamb A. K., Criado J. M., Pérez-Maqueda L. A., Popescu C., Sbirrazzuoli N. ICTAC Kinetics Committee recommendations for performing kinetic computations on thermal analysis data. *Thermochimica Acta*, **520**, pp. 1-19 (2011).
[13] Sainte Claire P. Degradation of PEO is solid state: a theoretical kinetic model. *Macromolecules*, **42**, pp. 3469-3482 (2009).